Journal of Mechanical Design, Volume 133, Issue 3

Time-Dependent Reliability Analysis for Function Generator Mechanisms

Dr. Junfu Zhang
School of Mechanical Engineering
Xihua University, P.R.China
zhang_junfu@126.com

Dr. Xiaoping Du*
Department of Mechanical and Aerospace Engineering
Missouri University of Science and Technology

***Corresponding Author**

dux@mst.edu
400 West 13th Street
Toomey Hall 290D
Rolla, MO 65401

Abstract

A function generator mechanism links its motion output and motion input with a desired functional relationship. The probability of realizing such functional relationship is the kinematic reliability. The time-dependent kinematic reliability is desired because it provides the reliability over the time interval where the functional relationship is defined. But the methodologies of time-dependent reliability are currently lacking for function generator mechanisms. We propose a mean value first passage method for time-dependent reliability analysis. With the assumption of normality for random dimension variables with small variances, the motion error becomes a non-stationary Gaussian process. We at first derive analytical equations for upcrossing and downcrossing rates and then develop a numerical procedure that integrates the two rates to obtain the kinematic reliability. A four-bar function generator is used as an example. The proposed method is accurate and efficient for normally distributed dimension variables with small variances.

1. Introduction

An important application of mechanisms is to generate functions, which link motion output and motion input with a functional relationship $y = f(x)$, where x is associated with motion input and y is associated with motion output. A mechanism that generates such a function is called a *function generator*. The motion error of a function generator is traditionally defined as the difference between the actual motion output and the desired motion output. Motion uncertainty might be a more precise definition for the motion error because the deviation from the desired motion can be caused by random dimensions. To comply with the traditional terminologies in the mechanism literature, however, we still use the motion error throughout this paper.

Tremendous efforts have been devoted to reducing the motion error [1-5], including the structural and mechanical types [6]. The former error is caused by the type of the mechanism, the number of design points, and the synthesis method used. It is the error calculated at the deterministic nominal dimensions and is therefore also deterministic. The latter error is stochastic because it is caused by random dimensions (tolerances), random clearances at joints, and random deformations of structural components. The structural error represents a bias, and the mechanical error indicates a random error. As a result, probabilistic methods are required to handle the mechanical error.

In the past decades, a large number of publications reported studies on the effects of uncertain parameters on the motion output with probabilistic and statistical methods [7-16]. The concept of reliability has also been introduced to kinematic analysis and synthesis [16]. Kinematic reliability is defined as the probability of the output member's position and/or orientation falling within a specified range from the desired position and/or orientation [17]. Kinematic reliability has applied to a wide range of mechanisms, such as close-chain mechanisms [18-21], open-loop robotic mechanisms [22-26], and flexible mechanisms [27-28].

For function generator mechanisms, the dominating reliability methods are Monte Carlo simulation (MCS) and the First Order Second Moment (FOSM) method. MCS can provide accurate solutions, but is computationally expensive. The FOSM is less accurate but much more efficient. For a linear function with normal variables, the solution from the FOSM is exact. Because the dimension variables of a mechanism are commonly assumed following normal distributions in the literature, in this work, we also use normal distributions for dimensional variables. If their standard deviations are small, the error function is near linear; and then the accuracy of the FOSM is quite satisfactory. The FOSM is therefore widely used for probabilistic mechanism analysis and synthesis [9, 18-19, 21].

Most kinematic reliability methods are only for the point reliability, which provides us with the likelihood of realizing the desired function only at a specific instant regardless whether the function has been realized or not before that instant. In many applications, it is more important to know the probability of realizing the desired function over the entire range (time period) of the input motion. Such a probability is time-dependent reliability or interval reliability, where the interval represents the range of the motion input where the desired function is defined.

In this work, we develop a method for interval kinematic reliability analysis for function generator mechanisms. The proposed method is accurate for function generator mechanisms that involve normal dimension variables with small variances. Such mechanisms are commonly encountered in engineering practices.

2. Background

2.1 Point kinematic reliability

Kinematic reliability is the probability that a mechanism realizes its desired motion within a specified error limit. For a function generator mechanism, its point kinematic reliability is the probability that the motion error at a specific motion input θ (or time instant) is within a specified tolerance range. Let the error function be

$$g(\mathbf{X}, \theta) = \psi(\mathbf{X}, \theta) - \psi_d(\theta) \tag{1}$$

where $\mathbf{X} = (X_1, \ldots, X_n)$ is an n-dimensional random vector, which include the dimension variables of the mechanism; $\psi(\mathbf{X}, \theta)$ and $\psi_d(\theta)$ are the actual motion output and desired motion output defined by the desired function $y = f(x)$, respectively. The relationship between $\psi_d(\theta)$ and $f(x)$ is described below [29].

Suppose the range of x is

$$x_0 \leqslant x \leqslant x_f \tag{2}$$

and the corresponding ranges of motion input θ and motion output ψ_d are

$$\theta_0 \leqslant \theta \leqslant \theta_f \tag{3}$$

and

$$\psi_0 \leqslant \psi_d \leqslant \psi_f \tag{4}$$

respectively.

Then

$$\psi_d(\theta) = \psi_0 + k_\psi \left[f\left(\frac{\theta - \theta_0}{k_\theta} + x_0 \right) - f(x_0) \right] \tag{5}$$

where

$$k_\theta = \frac{\theta_f - \theta_0}{x_f - x_0} \tag{6}$$

$$k_\psi = \frac{\psi_f - \psi_0}{f(x_f) - f(x_0)} \tag{7}$$

Eq. (5) converts the desired functional relationship $y = f(x)$ into the relationship between the motion input θ and motion output $\psi_d(\theta)$.

Eq. (1) contains both the structural and mechanical errors. To ensure the mechanism work properly, the motion error must be less than the allowable error ε.

$$|g(\mathbf{X}, \theta)| = |\psi(\mathbf{X}, \theta) - \psi_d(\theta)| \leqslant \varepsilon \tag{8}$$

Therefore, the point kinematic reliability R at θ is

$$R(\theta) = \Pr\left\{ |g(\mathbf{X}, \theta)| \leqslant \varepsilon \right\} = \Pr\left\{ -\varepsilon \leqslant g(\mathbf{X}, \theta) \leqslant \varepsilon \right\} \tag{9}$$

where $\Pr\{\cdot\}$ stands for a probability.

The point probability of failure is then given by

$$p_f(\theta) = \Pr\{|g(\mathbf{X},\theta)| > \varepsilon\} = \Pr\{g(\mathbf{X},\theta) > \varepsilon \cup g(\mathbf{X},\theta) < -\varepsilon\} \tag{10}$$

Note that the two events in the above equation are mutually exclusive.

The point reliability $R(\theta)$ tells us the likelihood that the mechanism functions properly at θ. This likelihood is the probability of success at instant θ regardless if the mechanism worked or failed before θ.

2.2 Time-dependent (interval) kinematic reliability

We are sometimes more interested in the interval kinematic reliability because it is concerned with the probability that the desired function is realized within the specified error ε over the range of the input motion $[\theta_0, \theta_f]$. The interval kinematic reliability is therefore computed by

$$\begin{aligned} R(\theta_0, \theta_f) &= \Pr\{|g(\mathbf{X},\theta)| \leqslant \varepsilon,\, \theta \in [\theta_0, \theta_f]\} \\ &= \Pr\{-\varepsilon \leqslant g(\mathbf{X},\theta) \leqslant \varepsilon,\, \theta \in [\theta_0, \theta_f]\} \end{aligned} \tag{11}$$

and the interval probability of failure is given by

$$\begin{aligned} p_f(\theta_0, \theta_f) &= \Pr\{|g(\mathbf{X},\theta)| > \varepsilon,\, \theta \in [\theta_0, \theta_f]\} \\ &= \Pr\{g(\mathbf{X},\theta) > \varepsilon \cup g(\mathbf{X},\theta) < -\varepsilon,\, \theta \in [\theta_0, \theta_f]\} \end{aligned} \tag{12}$$

Although the interval kinematic reliability has been rarely reported in the literature of mechanisms, many interval (time-dependent) reliability methods are available in the area of structural reliability. Time-dependent structural reliability problems involve time-dependent factors, such as decaying material properties and randomly varying load in time [30]. There are two basic types of methods for time-dependent reliability: extreme value methods [31-35] and first-passage methods [30, 33-34, 36-42].

The extreme value method uses the global maximum or minimum of the performance under consideration. As described previously, a failure occurs over a time interval if the performance is greater than or less than a threshold at any time instant over the time interval. The failure event is equivalent to the event that the extreme value over the time interval is greater than or less than the threshold. Therefore, if the distribution of the extreme value is identified, then a point reliability method can be used to solve for time-dependent reliability [31-32].

The first-passage method uses the first time when the performance exceeds or falls below a threshold. This method requires the calculation of the rate (crossing rate) of the likelihood that the performance exceeds or falls below the threshold. The most fundamental equation of solving the first-passage problem is the Rice formula [43]. Since the development of the Rice formula, many improvements have been made [44].

It is difficult to obtain the crossing rate for general stochastic processes [45]. A large number of methods have focused on the asymptotic integration approach to calculate the crossing rate [37-40]. For special stochastic processes, such as stationary Gaussian processes, an analytical outcrossing rate is available [33-34]. A new analytical derivation of the crossing rate has been reported recently [30] for general stochastic processes. This method is based on the First Order Reliability Method (FORM).

Unlike the general structural reliability problems, the error function $g(\mathbf{X}, \theta)$ in the kinematic reliability problem does not directly involve any time-dependent random variables – the random dimension variables $\mathbf{X}$ are time independent. However, as $g(\mathbf{X}, \theta)$

is a function of the time factor θ, it is indeed a stochastic process. Because the actual motion output $\psi(\mathbf{X}, \theta)$ and the desired motion output $\psi_d(\theta)$ are generally nonlinear functions of θ, the statistical moments of $g(\mathbf{X}, \theta) = \psi(\mathbf{X}, \theta) - \psi_d(\theta)$ are also generally time dependent. As a result, $g(\mathbf{X}, \theta)$ is a non-stationary stochastic process. The nonstationality of the error function makes the reliability analysis complicated. The common structural reliability analysis methods for stationary processes or Markovian processes are not applicable for the kinematic reliability problems.

3 Mean Value First Passage Method

The purpose of this work is to develop a method for solving for the time-dependent kinematic reliability. The method is based on the FOSM and the first-passage time methods and is therefore termed as the Mean Value First Passage (MVFP) method.

Suppose the means and standard deviations of $\mathbf{X}$ are $\mu_{\mathbf{X}} = (\mu_1, \ldots, \mu_n)$ and $\sigma_{\mathbf{X}} = (\sigma_1, \ldots, \sigma_n)$, respectively. The standard deviations $\sigma_{\mathbf{X}}$ are much smaller than the means $\mu_{\mathbf{X}}$ because the tolerances of dimensions are much smaller than the nominal dimension variables. As a result, the linearization of the error function $g(\mathbf{X}, \theta)$ at $\mu_{\mathbf{X}}$ can accurately represent $g(\mathbf{X}, \theta)$. We therefore linearize the error function at $\mu_{\mathbf{X}}$. After the linearization, we employ the concepts of upcrossing and downcrossing to estimate interval reliability $R(\theta_0, \theta_f)$. This requires knowing the upcrossing and downcrossing rates, which are derived in this section.

3.1 Linearization of the error function

The linearization is given by

$$g(\mathbf{X},\theta) \approx \hat{g}(\mathbf{X},\theta) = g(\mu_{\mathbf{X}},\theta) + \sum_{i=1}^{n} \left.\frac{\partial g(\mathbf{X},\theta)}{\partial X_i}\right|_{\mu_{\mathbf{X}}} (X_i - \mu_i) \tag{13}$$

The randomness in the dimension variables largely comes from manufacturing uncertainty, which can be described by a normal distribution; namely, $X_i \sim N(\mu_i, \sigma_i)$. Because the members of a mechanism are manufactured individually, the components of $\mathbf{X}$ are statistically independent. To simplify equations, we do transformation

$$X_i = \mu_i + \sigma_i U_i \tag{14}$$

where $U_i \sim N(0,1)$.

Then, the linearized function $\hat{g}(\mathbf{X},\theta)$ becomes

$$\hat{g}(\mathbf{U},\theta) = b_0(\theta) + \sum_{i=1}^{n} b_i(\theta) U_i \tag{15}$$

where $\mathbf{U} = (U_1, \ldots, U_n)$, $b_0(\theta) = g(\mu_{\mathbf{X}},\theta)$, and $b_i(\theta) = \left.\frac{\partial g(\mathbf{X},\theta)}{\partial X_i}\right|_{\mu_X} \sigma_i$.

Because $\hat{g}(\mathbf{U},\theta)$ is a linear combination of normal variables $\mathbf{U}$, $\hat{g}(\mathbf{U},\theta)$ is also normally distributed. Consequently, $\hat{g}(\mathbf{U},\theta)$ is a Gaussian process. The mean of $\hat{g}(\mathbf{U},\theta)$ is

$$\mu_g(\theta) = b_0(\theta) \tag{16}$$

and the standard deviation of $\hat{g}(\mathbf{U},\theta)$ is

$$\sigma_g(\theta) = \left[\sum_{i=1}^{n} b_i^2(\theta)\right]^{0.5} \tag{17}$$

Both of $\mu_g(\theta)$ and $\sigma_g(\theta)$ are functions of θ and are time-dependent. $\hat{g}(\mathbf{U},\theta)$ is therefore a non-stationary Gaussian process. Next, we employ the concept of upcrossing and downcrossing rates, which are based on the Poisson approximation for first-passage problems [30, 33], to make the reliability analysis possible.

3.2 Reliability analysis with the concepts of upcrossing and downcrossing

Fig. 1 shows the upcrossing and downcrossing events. The curve in the figure is a realization of the error function $g(\mathbf{X},\theta)$. When $g(\mathbf{X},\theta)$ is greater than the allowable error ε (upcrossing) or less than the other barrier $-\varepsilon$ (downcrossing), a failure occurs.

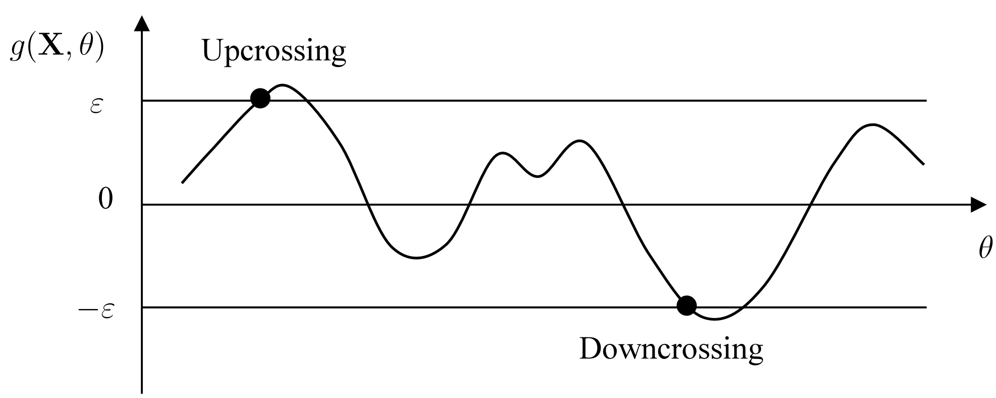

Fig. 1 Upcrossing and downcrossing events

The number of upcrossings or downcrossings is a random integer. The Poisson approximation of the first-passage problem assumes that the integer-valued process that counts the number of upcrossings or downcrossings is a Poisson process [33]. Under this assumption, the upcrossing and downcrossing events are statistically independent. This assumption has been commonly used in structural reliability analysis. Under this assumption, $R(\theta_0, \theta_f)$ is computed by

$$R(\theta_0, \theta_f) \approx R(\theta_0) \exp\left\{-\int_{\theta_0}^{\theta_f} \left[v^+(\theta) + v^-(\theta)\right] d\theta\right\} \tag{18}$$

where $v^+(\theta)$ and $v^-(\theta)$ are the upcrossing and downcrossing rates [30, 41], respectively; $R(\theta_0)$ is the initial point reliability at θ_0. With the linearization in Eq. (15) and from Eq. (9), $R(\theta_0)$ is computed by

$$R(\theta_0) = \Phi\left[\frac{\varepsilon - \mu_g(\theta_0)}{\sigma_g(\theta_0)}\right] - \Phi\left[\frac{-\varepsilon - \mu_g(\theta_0)}{\sigma_g(\theta_0)}\right] \tag{19}$$

where Φ is the cumulative distribution function (CDF) of a standard normal variable.

The upcrossing rate $v^+(\theta)$ is defined by [30]

$$v^+(\theta) = \lim_{\Delta\theta \to 0} \frac{w^+(\theta, \Delta\theta)}{\Delta\theta} \tag{20}$$

where $w^+(\theta, \Delta\theta)$ is the probability of upcrossing over $[\theta, \theta + \Delta\theta]$ and is given by

$$w^+(\theta, \Delta\theta) = \Pr\left\{g(\mathbf{X}, \theta) < \varepsilon \cap g(\mathbf{X}, \theta + \Delta\theta) > \varepsilon\right\} \tag{21}$$

$w^+(\theta, \Delta\theta)$ is the probability of upcrossing over $[\theta, \theta + \Delta\theta]$ on the condition that the error is less than ε at θ.

Similarly, the downcrossing rate is defined by

$$v^{-}(\theta) = \lim_{\Delta\theta \to 0} \frac{w^{-}(\theta, \Delta\theta)}{\Delta\theta} \tag{22}$$

where

$$w^{-}(\theta, \Delta\theta) = \Pr\left\{g(\mathbf{X}, \theta) > -\varepsilon \cap g(\mathbf{X}, \theta + \Delta\theta) < -\varepsilon\right\} \tag{23}$$

Next we follow the principles presented in [30] to derive analytical equations for $v^{+}(\theta)$ and $v^{-}(\theta)$.

3.3 Derivation of the upcrossing rate

As indicated in Eq. (21), $w^{+}(\theta, \Delta\theta)$ involves events $g(\mathbf{X}, \theta) < \varepsilon$ and $g(\mathbf{X}, \theta + \Delta\theta) > \varepsilon$. With the linearized function $\hat{g}(\mathbf{X}, \theta)$, we have

$$\begin{aligned} w^{+}(\theta, \Delta\theta) &\approx \Pr\left\{\hat{g}(\mathbf{X}, \theta) < \varepsilon \cap \hat{g}(\mathbf{X}, \theta + \Delta\theta) > \varepsilon\right\} \\ &= \Pr\left\{\hat{g}(\mathbf{X}, \theta) < \varepsilon \cap -\hat{g}(\mathbf{X}, \theta + \Delta\theta) < -\varepsilon\right\} \end{aligned} \tag{24}$$

To make the derivation easier, we transform $\hat{g}(\mathbf{X}, \theta)$ and $-\hat{g}(\mathbf{X}, \theta + \Delta\theta)$ into standard normal variables $U_g(\theta)$ and $U_g(\theta + \Delta\theta)$, respectively. The transformation is given by

$$U_g(\theta) = \frac{g(\mathbf{X}, \theta) - \mu_g(\theta)}{\sigma_g(\theta)} \tag{25}$$

and

$$\begin{aligned} U_g(\theta + \Delta\theta) &= \frac{-g(\mathbf{X}, \theta + \Delta\theta) - [-\mu_g(\theta + \Delta\theta)]}{\sigma_g(\theta + \Delta\theta)} \\ &= \frac{-g(\mathbf{X}, \theta + \Delta\theta) + \mu_g(\theta + \Delta\theta)}{\sigma_g(\theta + \Delta\theta)} \end{aligned} \tag{26}$$

Using Eqs. (15), (16) and (17), we have

$$U_g(\theta) = \frac{\sum_{i=1}^{n} b_i(\theta)U_i}{\left[\sum_{i=1}^{n} b_i^2(\theta)\right]^{0.5}} = \mathbf{a}(\theta)\cdot\mathbf{U} \tag{27}$$

where the dot means an inner product; and

$$\mathbf{a}(\theta) = \frac{\mathbf{b}(\theta)}{||\mathbf{b}(\theta)||} \tag{28}$$

in which

$$\mathbf{b}(\theta) = (b_1(\theta), \ldots, b_n(\theta)) \tag{29}$$

and $||\cdot||$ stands for the magnitude of a vector.

Similarly,

$$U_g(\theta+\Delta\theta) = -\frac{\sum_{i=1}^{n} b_i(\theta+\Delta\theta)U_i}{\left[\sum_{i=1}^{n} b_i^2(\theta+\Delta\theta)\right]^{0.5}} = -\mathbf{a}(\theta+\Delta\theta)\cdot\mathbf{U} \tag{30}$$

where

$$\mathbf{a}(\theta+\Delta\theta) = \frac{\mathbf{b}(\theta+\boldsymbol{\Delta}\theta)}{||\mathbf{b}(\theta+\boldsymbol{\Delta}\theta)||} \tag{31}$$

in which

$$\mathbf{b}(\theta+\Delta\theta) = (b_1(\theta+\Delta\theta), \ldots, b_n(\theta+\Delta\theta)) \tag{32}$$

$w^+(\theta, \Delta\theta)$ then becomes

$$\begin{aligned} w^+(\theta,\Delta\theta) &= \Pr\{(\mu_g(\theta) + \sigma_g(\theta)U_g(\theta) < \varepsilon)\cap \\ &\quad (-\mu_g(\theta+\Delta\theta) + \sigma_g(\theta+\Delta\theta)U_g(\theta+\Delta\theta) < -\varepsilon)\} \\ &= \Pr\left\{U_g(\theta) < \beta_+(\theta) \cap U_g(\theta+\Delta\theta) < -\beta_+(\theta+\Delta\theta)\right\} \end{aligned} \tag{33}$$

where

$$\beta_+(\theta) = \frac{\varepsilon - \mu_g(\theta)}{\sigma_g(\theta)} \tag{34}$$

and

$$\beta_{+}(\theta+\Delta\theta) = \frac{\varepsilon - \mu_g(\theta+\Delta\theta)}{\sigma_g(\theta+\Delta\theta)} \tag{35}$$

Because the joint distribution of $U_g(\theta)$ and $U_g(\theta+\Delta\theta)$ is a bivariate normal distribution, $w^{+}(\theta,\Delta\theta)$ can be computed by the bivariate CDF as follows:

$$w^{+}(\theta,\Delta\theta) = \Phi_2[\beta_{+}(\theta), -\beta_{+}(\theta+\Delta\theta), \rho(\theta,\theta+\Delta\theta)] \tag{36}$$

where Φ_2 is the bivariate CDF of normal variables, which can be obtained from its corresponding PDF

$$\phi_2(x,y,\rho) = \frac{1}{2\pi\sqrt{1-\rho^2}} \exp\left[-\frac{1}{2}\frac{x^2-2\rho xy+y^2}{1-\rho^2}\right] \tag{37}$$

where ρ is the correlation coefficient. Using Eq. (27) and (30), we obtain

$$\rho(\theta,\theta+\Delta\theta) = -\mathbf{a}(\theta)\cdot\mathbf{a}(\theta+\Delta\theta) \tag{38}$$

After obtaining $w^{+}(\theta,\Delta\theta)$, we now take its limit to derive the equation of the upcrossing rate. Because $w^{+}(\theta,0)=0$,

$$v^{+}(\theta) = \lim_{\Delta\theta\to 0}\frac{w^{+}(\theta,\Delta\theta)-w^{+}(\theta,0)}{\Delta\theta} = \left.\frac{\partial w^{+}(\theta,\Delta\theta)}{\partial\Delta\theta}\right|_{\Delta\theta=0} \tag{39}$$

We use the following two equations given in [30] to derive the derivative of $w^{+}(\theta,\Delta\theta)$:

$$\frac{\partial\Phi_2(x,y,\rho)}{\partial y} = \phi(y)\Phi\left(\frac{x-\rho y}{\sqrt{1-\rho^2}}\right) \tag{40}$$

where $\phi(\cdot)$ is the probability density function (PDF) of a standard normal variable, and

$$\frac{\partial \Phi_2(x,y,\rho)}{\partial \rho} = \phi_2(x,y,\rho) \tag{41}$$

Differentiating $w^+(\theta, \Delta\theta)$ in Eq. (36), we obtain

$$\frac{\partial w^+(\theta,\Delta\theta)}{\partial \Delta\theta} = I_1(\theta,\Delta\theta) + I_2(\theta,\Delta\theta) \tag{42}$$

where

$$\begin{aligned} I_1(\theta,\Delta\theta) &= -\frac{\partial \Phi_2\left[\beta_+(\theta), -\beta_+(\theta+\Delta\theta), \rho(\theta,\theta+\Delta\theta)\right]}{\partial\left[\beta_+(\theta+\Delta\theta)\right]}\beta_+'(\theta+\Delta\theta) \\ &= -\phi[\beta_+(\theta+\Delta\theta)]A\beta_+'(\theta+\Delta\theta) \end{aligned} \tag{43}$$

in which

$$A = \Phi\left[\frac{\beta_+(\theta)+\rho(\theta,\theta+\Delta\theta)\beta_+(\theta+\Delta\theta)}{\sqrt{1-\rho^2(\theta,\theta+\Delta\theta)}}\right] \tag{44}$$

and

$$\begin{aligned} I_2(\theta,\Delta\theta) &= \frac{\partial \Phi_2\left[\beta_+(\theta), -\beta_+(\theta+\Delta\theta), \rho(\theta,\theta+\Delta\theta)\right]}{\partial \rho(\theta+\Delta\theta)}\rho'(\theta+\Delta\theta) \\ &= \phi_2\left[\beta_+(\theta), -\beta_+(\theta+\Delta\theta), \rho(\theta,\theta+\Delta\theta)\right]\rho'(\theta+\Delta\theta) \end{aligned} \tag{45}$$

The upcrossing rate $v^+(\theta)$ is then given by

$$v^+(\theta) = \left.\frac{\partial w^+(\theta,\Delta\theta)}{\partial \Delta\theta}\right|_{\Delta\theta=0} = \lim_{\Delta\theta\to 0}[I_1(\theta,\Delta\theta) + I_2(\theta,\Delta\theta)] \tag{46}$$

To get the limits of $I_1(\theta, \Delta\theta)$ and $I_2(\theta, \Delta\theta)$, by differentiating Eq. (28), we obtain

$$\mathbf{a}(\theta) \cdot \mathbf{a}'(\theta) = 0 \tag{47}$$

Taking differentiation again, we get

$$[\mathbf{a}'(\theta)]^2 + \mathbf{a}(\theta) \cdot \mathbf{a}''(\theta) = 0 \tag{48}$$

Then

$$\mathbf{a}(\theta) \cdot \mathbf{a}''(\theta) = -[\mathbf{a}'(\theta)]^2 = -||\mathbf{a}'(\theta)||^2 \tag{49}$$

Differentiating Eq. (38), we obtain

$$\lim_{\Delta\theta \to 0} \rho'(\theta, \theta + \Delta\theta) = \mathbf{a}(\theta) \cdot \mathbf{a}'(\theta) = 0 \tag{50}$$

$$\lim_{\Delta\theta \to 0} \rho''(\theta, \theta + \Delta\theta) = \mathbf{a}(\theta) \cdot \mathbf{a}''(\theta) = -||\mathbf{a}'(\theta)||^2 \tag{51}$$

These two limits will be used later on. To easily obtain the limit given in Eq. (39), we also define

$$M = \lim_{\Delta\theta \to 0} \left[-\frac{\sqrt{1 - \rho^2(\theta, \theta + \Delta\theta)}}{\rho'(\theta, \theta + \Delta\theta)} \right] \tag{52}$$

we then obtain

$$\begin{aligned}
M &= \lim_{\Delta\theta\to 0}\left[-\frac{\sqrt{1-\rho^2(\theta,\theta+\Delta\theta)}}{\rho'(\theta,\theta+\Delta\theta)}\right] \\
&= \lim_{\Delta\theta\to 0}\frac{\sqrt{1-[\mathbf{a}(\theta)\cdot\mathbf{a}(\theta,\theta+\Delta\theta)]^2}}{\mathbf{a}(\theta)\cdot\mathbf{a}'(\theta,\theta+\Delta\theta)} \\
&\overset{L'Hopital}{=} \lim_{\Delta\theta\to 0}\frac{[\mathbf{a}(\theta)\cdot\mathbf{a}(\theta,\theta+\Delta\theta)][\mathbf{a}(\theta)\cdot\mathbf{a}'(\theta,\theta+\Delta\theta)]}{[\mathbf{a}(\theta)\cdot\mathbf{a}''(\theta,\theta+\Delta\theta)]\sqrt{1-[\mathbf{a}(\theta)\cdot\mathbf{a}(\theta,\theta+\Delta\theta)]^2}} \\
&= \frac{[\mathbf{a}(\theta)\cdot\mathbf{a}(\theta)]}{[\mathbf{a}(\theta)\cdot\mathbf{a}''(\theta)]}\lim_{\Delta\theta\to 0}\frac{[\mathbf{a}(\theta)\cdot\mathbf{a}'(\theta,\theta+\Delta\theta)]}{\sqrt{1-[\mathbf{a}(\theta)\cdot\mathbf{a}(\theta,\theta+\Delta\theta)]^2}} \\
&= \frac{1}{||\mathbf{a}'(\theta)||^2}\frac{1}{M}
\end{aligned} \tag{53}$$

The above limit involves a zero-divided-by-zero form, and the L' Hopital's Rule is therefore used. Then

$$M = \frac{1}{||\mathbf{a}'(\theta)||} \tag{54}$$

The limit of A in Eq. (43) for $I_1(\theta,\Delta\theta)$ is

$$\begin{aligned}
\lim_{\Delta\theta\to 0} A &= \lim_{\Delta\theta\to 0}\frac{\beta_+(\theta)+\rho(\theta,\theta+\Delta\theta)\beta_+(\theta+\Delta\theta)}{\sqrt{1-\rho^2(\theta,\theta+\Delta\theta)}} \\
&\overset{L'Hopital}{=} \lim_{\Delta\theta\to 0}\frac{\rho'(\theta,\theta+\Delta\theta)\beta_+(\theta+\Delta\theta)+\rho(\theta,\theta+\Delta\theta)\beta_+'(\theta+\Delta\theta)}{-\rho(\theta,\theta+\Delta\theta)\rho'(\theta,\theta+\Delta\theta)}\sqrt{1-\rho^2(\theta,\theta+\Delta\theta)} \\
&= \beta_+'(\theta)\lim_{\Delta\theta\to 0}-\frac{\sqrt{1-\rho^2(\theta,\theta+\Delta\theta)}}{\rho'(\theta,\theta+\Delta\theta)} \\
&= \beta_+'(\theta)\frac{1}{M} = \frac{\beta_+'(\theta)}{||\mathbf{a}'(\theta)||}
\end{aligned}$$

(55)

The limit of $I_1(\theta,\Delta\theta)$ is therefore given by

$$\begin{aligned}\lim_{\Delta\theta\to 0} I_1(\theta,\Delta\theta) &= \lim_{\Delta\theta\to 0} -\phi[\beta_+(\theta+\Delta\theta)]A\beta'_+(\theta+\Delta\theta) \\ &= -\beta'_+(\theta)\phi[\beta_+(\theta)]\Phi\left[\frac{\beta'_+(\theta)}{||\mathbf{a}'(\theta)||}\right]\end{aligned} \tag{56}$$

We now derive the limit of $I_2(\theta,\Delta\theta)$. According to Eqs. (45) and (37),

$$I_2(\theta,\Delta\theta) = \frac{\rho'(\theta,\theta+\Delta\theta)}{\sqrt{1-\rho^2(\theta,\theta+\Delta\theta)}}\frac{1}{2\pi}\exp(B) \tag{57}$$

where

$$B = -\frac{1}{2}\frac{\beta_+^2(\theta) - 2\rho(\theta,\theta+\Delta\theta)\beta_+(\theta)\beta(\theta+\Delta\theta) + \beta_+^2(\theta+\Delta\theta)}{1-\rho^2(\theta,\theta+\Delta\theta)} \tag{58}$$

The limit of B is

$$\begin{aligned}\lim_{\Delta\theta\to 0} B &= \lim_{\Delta\theta\to 0} -\frac{1}{2}\frac{\beta_+^2(\theta) - 2\rho(\theta,\theta+\Delta\theta)\beta_+(\theta)\beta(\theta+\Delta\theta) + \beta_+^2(\theta+\Delta\theta)}{1-\rho^2(\theta,\theta+\Delta\theta)} \\ &= -\frac{1}{2}\left[\beta_+^2(\theta) + \frac{\beta_+'^2(\theta)}{||\mathbf{a}'(\theta)||^2}\right]\end{aligned} \tag{59}$$

The limit of $I_2(\theta,\Delta\theta)$ is therefore given by

$$\lim_{\Delta\theta\to 0} I_2(\theta,\Delta\theta) = \frac{1}{M}\lim_{\Delta\theta\to 0}\frac{1}{2\pi}\exp(B) = \|\mathbf{a}'(\theta)\|\,\phi(\beta_+(\theta))\phi\left(\frac{\beta'_+(\theta)}{\|\mathbf{a}'(\theta)\|}\right) \tag{60}$$

The L' Hopital's Rule is used twice in deriving the above equation. Then $v^+(\theta)$ is

$$\begin{aligned}v^+(\theta) &= \lim_{\Delta\theta\to 0} I_1(\theta,\Delta\theta) + \lim_{\Delta\theta\to 0} I_2(\theta,\Delta\theta) \\ &= \|\mathbf{a}'(\theta)\|\,\phi(\beta_+(\theta))\left\{\phi\left[\frac{\beta'_+(\theta)}{\|\mathbf{a}'(\theta)\|}\right] - \frac{\beta'_+(\theta)}{\|\mathbf{a}'(\theta)\|}\Phi\left[\frac{\beta'_+(\theta)}{||\mathbf{a}'(\theta)||}\right]\right\}\end{aligned} \tag{61}$$

Therefore, the upcrossing rate is obtained as

$$v^{+}(\theta) = ||\mathbf{a}'(\theta)||\phi[\beta_{+}(\theta)]\Psi\left[\frac{\beta_{+}'(\theta)}{||\mathbf{a}'(\theta)||}\right] \tag{62}$$

where $\Psi(x) = \phi(x) - x\Phi(-x)$. The result is the same as in [30].

3.4 Derivation of the downcrossing rate

To avoid repeating deriving similar equations, we can use the results for the upcrossing rate. What we need is to perform a simple transformation that converts a downcrossing event to an upcrossing event. The idea is that the upcrossing of function $g(\mathbf{X}, \theta)$ is the downcrossing of function $-g(\mathbf{X}, \theta)$. We therefore replace $g(\mathbf{X}, \theta)$ with $-g(\mathbf{X}, \theta)$ in the equations for the upcrossing rate.

As shown in Eq. (22), the downcrossing rate $v^{-}(\theta)$ is defined by

$$v^{-}(\theta) = \lim_{\Delta\theta \to 0} \frac{\Pr\{g(\mathbf{X}, \theta) > -\varepsilon \cap g(\mathbf{X}, \theta + \Delta\theta) < -\varepsilon\}}{\Delta\theta} = \lim_{\Delta\theta \to 0} \frac{w^{-}(\theta, \Delta\theta)}{\Delta\theta} \tag{63}$$

where

$$w^{-}(\theta, \Delta\theta) = \Pr\{g(\mathbf{X}, \theta) > -\varepsilon \cap g(\mathbf{X}, \theta + \Delta\theta) < -\varepsilon\} \tag{64}$$

It is equivalent to

$$\begin{aligned} w^{-}(\theta, \Delta\theta) &= \Pr\{-g(\mathbf{X}, \theta) < \varepsilon \cap -g(\mathbf{X}, \theta + \Delta\theta) > \varepsilon\} \\ &= \Pr\{\tilde{g}(\mathbf{X}, \theta) < \varepsilon \cap \tilde{g}(\mathbf{X}, \theta + \Delta\theta) > \varepsilon\} \end{aligned} \tag{65}$$

where

$$\tilde{g}(\mathbf{X}, \theta) = -g(\mathbf{X}, \theta) \tag{66}$$

and

$$\tilde{g}(\mathbf{X}, \theta + \Delta\theta) = -g(\mathbf{X}, \theta + \Delta\theta)) \tag{67}$$

Now Eq. (65) is in the same form as Eq. (21). We can use Eq. (21) to get the downcrossing rate as

$$v^-(\theta) = ||\mathbf{a}^{'}(\theta)||\phi[\beta_-(\theta)]\Psi\left[\frac{\beta_-^{'}(\theta)}{||\mathbf{a}^{'}(\theta)||}\right] \tag{68}$$

where

$$\beta_-(\theta) = \frac{\varepsilon - \mu_{\tilde{g}}(\theta)}{\sigma_{\tilde{g}}(\theta)} = \frac{\varepsilon + \mu_g(\theta)}{\sigma_g(\theta)} \tag{69}$$

The following equations are used in deriving Eq. (68):

$$\mu_{\tilde{g}} = -\mu_g \tag{70}$$

and

$$\sigma_{\tilde{g}} = \sigma_g \tag{71}$$

3.5 Mechanism analysis

The equations of the upcrossing and downcrossing rates depend on the derivatives of the error function with respect to $\mu_{\mathbf{X}}$. The derivatives can be obtained analytically from mechanism analysis. Let the loop equation of the mechanism be

$$\mathbf{F}(\mathbf{X}, \theta, \mathbf{h}(\mathbf{X}, \theta)) = \mathbf{0} \tag{72}$$

where $\mathbf{h}$ is a m-dimensional output vector, which includes the motion output $\psi(\mathbf{X}, \theta)$ in Eq. (1).

We now apply the direct linearization method (DLM) [46] to get the derivatives of the error function. From Eq. (72), we can obtain the sensitivity (Jacobi) matrix $\mathbf{J}(\theta)$

$$\mathbf{J}(\theta) = -[\mathbf{C}(\theta)]^{-1}\mathbf{D}(\theta) \tag{73}$$

where $\mathbf{C}_{ij}(\theta) = \left.\frac{\partial \mathbf{F}_i(\mathbf{X},\theta,\mathbf{h}(\mathbf{X},\theta))}{\partial \mathbf{h}_j(\mathbf{X},\theta)}\right|_{\mu_X}$, $\mathbf{D}_{ik}(\theta) = \left.\frac{\partial \mathbf{F}_i(\mathbf{X},\theta,\mathbf{h}(\mathbf{X},\theta))}{\partial \mathbf{X}_k}\right|_{\mu_X}$, and the size of $\mathbf{J}(\theta)$ is $m \times n$.

$\mathbf{C}(\theta)$ and $\mathbf{D}(\theta)$ are analytically available from the loop equation in Eq. (72). Assume that the s-th component of $\mathbf{h}(\mathbf{X},\theta)$ is the motion output $\psi(\mathbf{X},\theta)$. Then $b_i(\theta)$ in Eq. (15) is given by

$$b_i(\theta) = \mathbf{J}_{si}(\theta)\sigma_i \quad (i = 1, \cdots, n) \tag{74}$$

Differentiating $b_i(\theta)$ with respect to θ, we obtain $b_i'(\theta)$ and then vector $\mathbf{a}'(\theta)$ in Eq. (62) as follows:

$$\mathbf{a}'(\theta) = \frac{\sigma_g(\theta)\mathbf{b}'(\theta) - \mathbf{b}\sigma_g'(\theta)}{\sigma_g^2(\theta)} \tag{75}$$

in which

$$\sigma_g'(\theta) = \frac{1}{\sigma_g(\theta)}\mathbf{b}(\theta) \cdot \mathbf{b}'(\theta) \tag{76}$$

where $\mathbf{b}'(\theta) = (b_1'(\theta), \ldots, b_n'(\theta))$

With the above analytical equations, $\beta_+(\theta)$ and $\beta_-(\theta)$ are

$$\beta'_{+}(\theta) = \frac{-\sigma_g(\theta)\mu'_g(\theta) - [\varepsilon - \mu_g(\theta)]\sigma'_g(\theta)}{\sigma_g^2(\theta)} \tag{77}$$

and

$$\beta'_{-}(\theta) = \frac{\sigma_g(\theta)\mu'_g(\theta) - [\varepsilon + \mu_g(\theta)]\sigma'_g(\theta)}{\sigma_g^2(\theta)} \tag{78}$$

in which

$$\mu'_g(\theta) = \left.\frac{d\psi(\mathbf{X},\theta)}{d\theta}\right|_{\mu_X} - \frac{d\psi_d(\theta)}{d\theta} \tag{79}$$

The above equations ensure that the upcrossing and downcrossing rates be analytically available.

3.6 Numerical procedure

Having obtained all the analytical equations, we now summarize the procedure of computing interval kinematic reliability (Fig. 2).

Step 1. Input parameters, such as the mean and standard deviations of dimension variables, the allowable error limit, and the ranges of the motion input and motion output.

Step 2. Perform mechanism analysis to obtain the motion error function $g(\mathbf{X},\theta)$. Then linearize $g(\mathbf{X},\theta)$ at $\mu_{\mathbf{X}}$ using Eq. (13). Derive equations for $\mu_g(\theta)$ using Eq. (16) and its derivative $\mu'_g(\theta)$ using Eq. (79); standard deviation $\sigma_g(\theta)$ using Eq. (17), and its derivative $\sigma'_g(\theta)$ using Eq. (76); reliability index $\beta(\theta)$ using Eq. (34) or Eq. (69), and its derivative $\beta'(\theta)$ using Eq. (77) or Eq. (78); and the unit vector $\mathbf{a}(\theta)$ using Eq. (28), and its derivative $\mathbf{a}'(\theta)$ using Eq. (75).

Step 3. Calculate the initial point reliability $R(\theta_0)$ using Eq. (18).

Step 4. Find the upcrossing and downcrossing rates $v^+(\theta)$ and $v^-(\theta)$ using Eqs. (62) and (68), respectively.

Step 5. Calculate reliability $R(\theta_0, \theta_f)$ by integrating $v^+(\theta)$ and $v^-(\theta)$ over the input range $[\theta_0, \theta_f]$ and multiplying the integral by $R(\theta_0)$ using Eq. (18).

4 Numerical Example

In this section, we present the application of the MVFP method for a planar four-bar function generator mechanism.

4.1 Problem statement

The mechanism is shown in Fig.3. The crank *AB* is the input member with the input angle θ, and the rocker *CD* is the output member with the output angle ψ. R_1, R_2, R_3, and R_4 are the dimensions of the mechanism. In this study, we consider two cases where the standard deviations (std) in Case 1 are larger than those in Case 2.

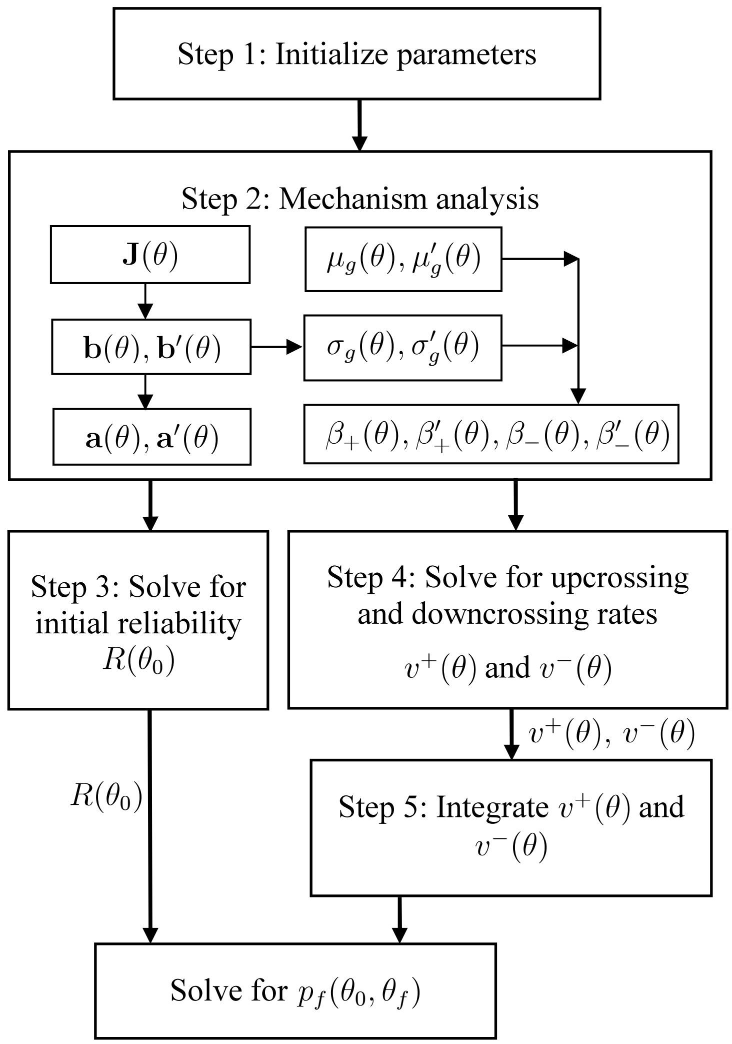

Fig. 2 Flowchart of time-dependent mechanism reliability analysis

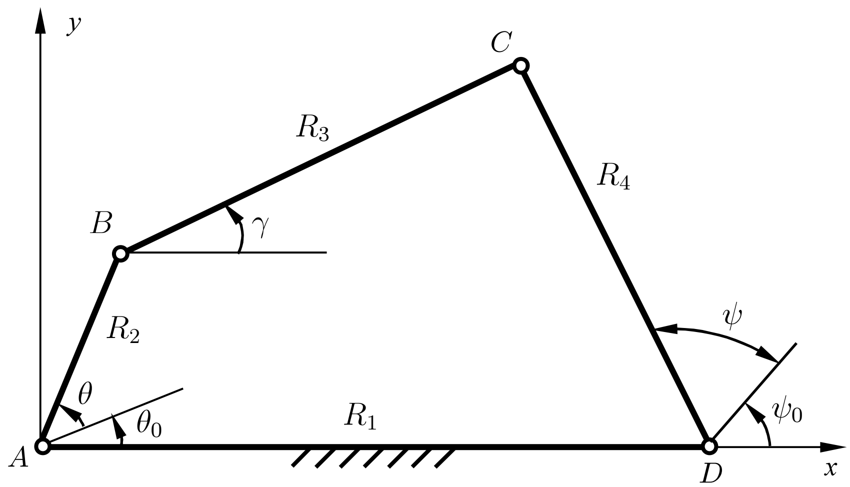

Fig. 3 Four-bar function generator mechanism

Two desired functions are involved. The first one is a sine function defined by $y = \sin x$ with $x \in [x_0, x_f] = [0, 90°]$. The range of the input angle is $[\theta_0, \theta_1] = [97°, 217°]$, and the range of the output angle is $[\psi_0, \psi_f] = [60°, 120°]$. According to Eq. (5), the relationship between the desired output ψ_d and input θ is $\psi_d(\theta) = 60° + 60° \sin[\frac{3}{4}(\theta - 97°)]$. The distributions of the dimension variables are given in Table 1. The second desired function is a logarithm function defined by $y = \log_{10} x$ with $x \in [x_0, x_f] = [1, 2]$. The ranges of the input and output angles are $[\theta_0, \theta_1] = [45°, 105°]$ and $[\psi_0, \psi_f] = [0°, 60°]$, respectively. The relationship between the desires output ψ_d and input θ is $\psi_d(\theta) = \frac{60° \log_{10}\left(\frac{\theta + 15°}{60°}\right)}{\log_{10}^{2}}$. The distributions of the dimension variables are given in Table 2.

Table 1 Random dimensions for the sine function generator

Variable	Mean (mm)	Standard deviation (mm)		Distribution
		Case 1 (larger std)	Case 2 (smaller std)	
R_1	$\mu_1 = 100.0$	$\sigma_1 = 0.05$	$\sigma_1 = 0.025$	Normal
R_2	$\mu_2 = 55.5$	$\sigma_2 = 0.05$	$\sigma_2 = 0.025$	Normal
R_3	$\mu_3 = 144.1$	$\sigma_3 = 0.05$	$\sigma_3 = 0.025$	Normal
R_4	$\mu_4 = 72.5$	$\sigma_4 = 0.05$	$\sigma_4 = 0.025$	Normal

Table 2 Random dimensions for the log function generator

Variable	Mean (mm)	Standard deviation (mm)		Distribution
		Case 1 (larger std)	Case 2 (smaller std)	
R_1	$\mu_1 = 100.0$	$\sigma_1 = 0.05$	$\sigma_1 = 0.025$	Normal
R_2	$\mu_2 = 79.5$	$\sigma_2 = 0.05$	$\sigma_2 = 0.025$	Normal
R_3	$\mu_3 = 203.0$	$\sigma_3 = 0.05$	$\sigma_3 = 0.025$	Normal
R_4	$\mu_4 = 150.8$	$\sigma_4 = 0.05$	$\sigma_4 = 0.025$	Normal

4.2 Kinematic analysis of the four-bar function generator

The loop-closure equations of the four-bar mechanism are given by

$$\mathbf{F}(\mathbf{X}, \theta, \mathbf{h}) = \begin{bmatrix} R_2 \cos\theta + R_3 \cos\gamma(\mathbf{X}, \theta) - R_1 - R_4 \cos\psi(\mathbf{X}, \theta) \\ R_2 \sin\theta + R_3 \sin\gamma(\mathbf{X}, \theta) - R_4 \sin\psi(\mathbf{X}, \theta) \end{bmatrix} = \mathbf{0} \tag{80}$$

where $\mathbf{X} = (R_1, R_2, R_3, R_4)$ and $\mathbf{h} = [\gamma(\mathbf{X}, \theta), \psi(\mathbf{X}, \theta)]$.

Solving the above equations, we obtain the closed-form solution

$$\psi(\mathbf{X}, \theta) = 2 \arctan\left(\frac{-E \pm \sqrt{E^2 + D^2 - F^2}}{F - D} \right) \tag{81}$$

where $D = 2R_4(R_1 - R_2 \cos\theta)$, $E = -2R_2 R_4 \sin\theta$ and
$F = R_1^2 + R_2^2 + R_4^2 - R_3^2 - 2R_1 R_2 \cos\theta$.

As explained previously, the motion error function is close to linear around the mean values of the dimension variables with small standard deviations. Using the direct linearization method in Eqs. (73) and (74), we get vectors $\mathbf{b}(\theta)$ and $\mathbf{b}'(\theta)$

$$\mathbf{b}(\theta) = \frac{\sigma_X}{R_4 \sin(\gamma - \psi)}[-\cos\gamma, \cos(\theta - \gamma), 1, -\cos(\gamma - \psi)] \tag{82}$$

and

$$\mathbf{b}'(\theta) = \frac{\mathbf{Q}^{\mathrm{T}} \cdot \sigma_X}{R_4 \sin^2(\gamma - \psi)} \tag{83}$$

in which

$$\mathbf{Q} = \begin{bmatrix} \cos\psi\frac{d\gamma}{d\theta} - \cos\gamma\cos(\gamma-\psi)\frac{d\psi}{d\theta} \\ \sin(\theta-\gamma)\sin(\gamma-\psi) + \cos(\theta-\psi)\frac{d\gamma}{d\theta} - \cos(\theta-\gamma)\cos(\gamma-\psi)\frac{d\psi}{d\theta} \\ \cos(\gamma-\psi)(\frac{d\gamma}{d\theta} - \frac{d\psi}{d\theta}) \\ \frac{d\gamma}{d\theta} - \frac{d\psi}{d\theta} \end{bmatrix}$$

$$\frac{d\gamma}{d\theta} = \frac{R_2 R_3 \sin(\theta - \gamma) - R_1 R_2 \sin(\theta)}{R_2 R_3 \sin(\theta - \gamma) - R_1 R_3 \sin(\gamma)}$$

$$\frac{d\psi}{d\theta} = \frac{R_2 R_4 \sin(\theta - \psi) - R_1 R_2 \sin(\theta)}{R_2 R_4 \sin(\theta - \psi) - R_1 R_4 \sin(\psi)}$$

where γ and ψ stand for $\gamma(\mu_{\mathbf{X}}, \theta)$ and $\psi(\mu_{\mathbf{X}}, \theta)$, respectively.

4.3 Reliability analysis

We use the following equations for our computation: Eqs. (1), (16), (79), and (81) for $\mu_g(\theta)$ and $\mu_g'(\theta)$; Eqs. (82) and (83) for $\mathbf{b}(\theta)$ and $\mathbf{b}'(\theta)$; Eqs. (17) and (76) for $\sigma_g(\theta)$ and $\sigma_g'(\theta)$; Eqs. (34) and (69) for $\beta_+(\theta)$ and $\beta_-(\theta)$; Eqs. (75), (77), and (78) for $\mathbf{a}'(\theta)$,

$\beta'_+(\theta)$, and $\beta'_-(\theta)$. Eqs. (62) and (68) for the upcrossing and downcrossing rates; and Eq. (18) for interval reliability.

Monte Carlo simulation (MCS) is also used with a large sample size of 10^7. The percentage error is defined by

$$\text{Error} = \frac{\left|p_f - p_f^{\text{MCS}}\right|}{p_f^{\text{MCS}}} \times 100\% \tag{84}$$

where p_f is the interval probability of failure over the input angle range $[\theta_0, \theta_f]$ from the MVFP method, and p_f^{MCS} is its counterpart from MCS.

The results with several allowable errors for the sine function generator are given in Table 3 (Case 1) and Table 4 (Case 2) and plotted in Figs. 4 (Case 1) and 5 (Case 2). The results indicate that the solutions of the present method are very close to those of MCS and are therefore accurate. The results also show that the MVFP method is more accurate in Case 2 than in Case 1. This indicates that the MVFP method is more accurate with smaller standard deviations.

The number of mechanism analyses is determined by the adaptive Simpson quadrature method with a tolerance of 10^{-5}. The numbers of function calls by the MVFP method are listed in Table 3 and Table 4, which indicate that the MVFP method is much more efficient than MCS.

Table 3 p_f for the sine function generator (Case 1)

$\varepsilon(°)$	MVFP	MCS		Error	Number of
	p_f	p_f^{MCS}	95% confidence interval	(%)	function calls
0.70	0.9799	1.00	(0.9997, 1.0)	2.0	86
0.75	0.8977	0.9971	(0.9968, 0.9974)	10.0	46
0.80	0.6901	0.7299	(0.7297, 0.7301)	5.46	38
0.85	0.4069	0.4103	(0.4102, 0.4105)	0.84	30
0.90	0.1737	0.1738	(0.1738, 0.1739)	0.08	26
0.95	5.1123×10^{-2}	5.1195×10^{-2}	$(5.1178, 5.1211)\times10^{-2}$	0.14	14
1.00	9.9702×10^{-3}	1.0049×10^{-2}	$(1.0046, 1.0052)\times10^{-2}$	0.78	14
1.05	1.2628×10^{-3}	1.2811×10^{-3}	$(1.2807, 1.2815)\times10^{-3}$	1.43	14
1.10	1.0241×10^{-4}	1.0440×10^{-4}	$(1.0437, 1.0443)\times10^{-4}$	1.91	14

Table 4 p_f for the sine function generator (Case 2)

$\varepsilon(°)$	MVFP	MCS		Error	Number of
	p_f	p_f^{MCS}	95% confidence interval	(%)	function calls
0.70	0.9999	1.00	(0.9998, 1.0)	0.0	58
0.75	0.9892	1.00	(0.9997, 1.0)	1.18	42
0.80	0.81255	0.8130	(0.8128, 0.8132)	0.06	26
0.85	0.3090	0.3089	(0.3088, 0.3089)	0.04	14
0.90	2.9771×10^{-2}	2.9800×10^{-2}	$(2.9793, 2.9808)\times10^{-2}$	0.10	14
0.95	5.3844×10^{-4}	5.4510×10^{-4}	$(5.4497, 5.4523)\times10^{-4}$	1.22	14
0.975	3.7107×10^{-5}	3.6700×10^{-4}	$(3.6691, 3.6709)\times10^{-4}$	1.11	14

The interval probabilities of failure for the log function generator are plotted in Figs. 6 and 7. The results also show that the MVFP method is accurate and is efficient. Same conclusion can be drawn as those for the sine function generator.

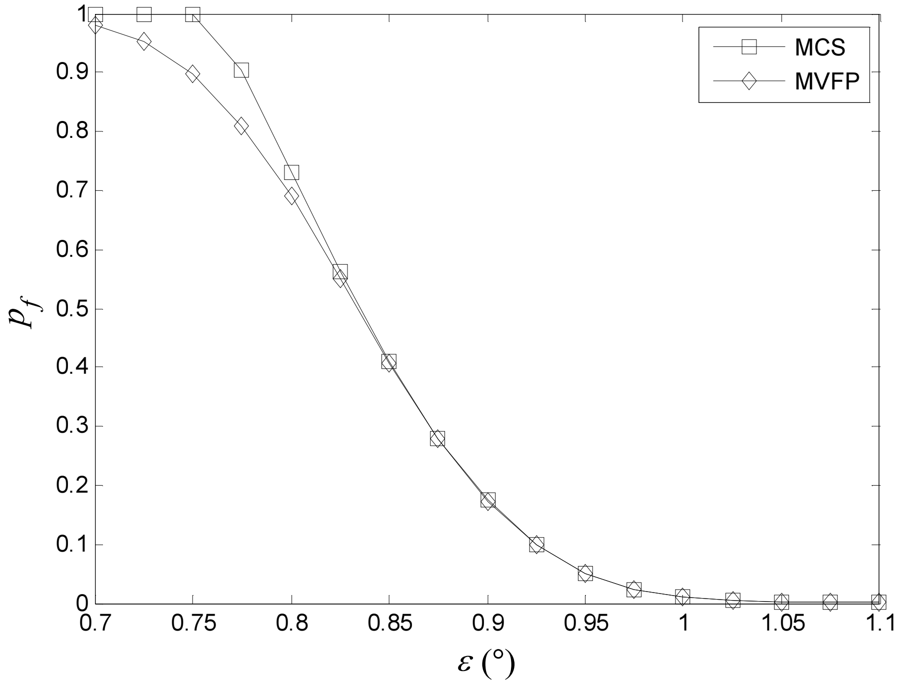

Fig. 4 p_f **of the sine function generator (Case 1)**

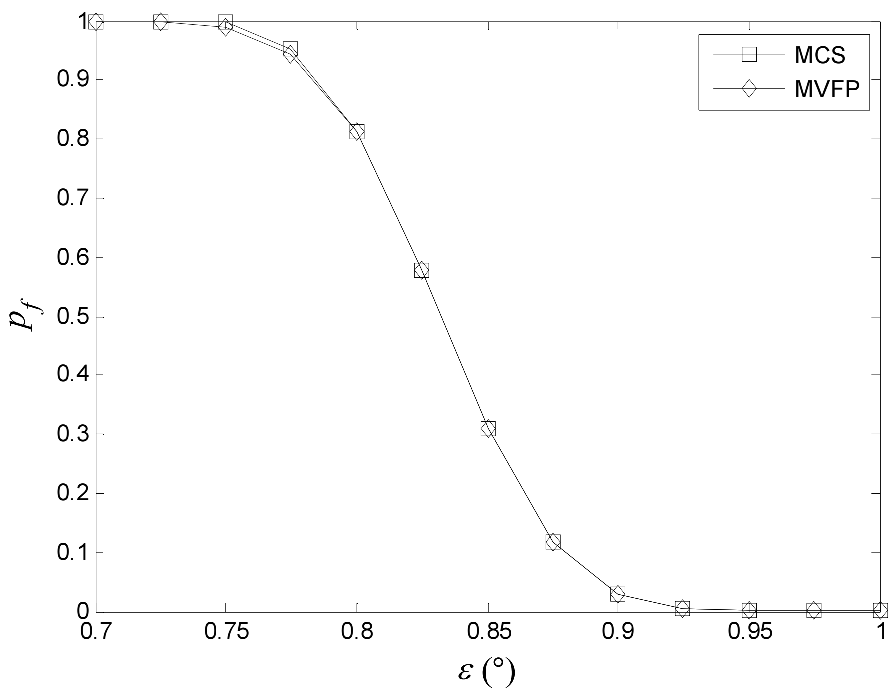

Fig. 5 p_f **of the sine function generator (Case 2)**

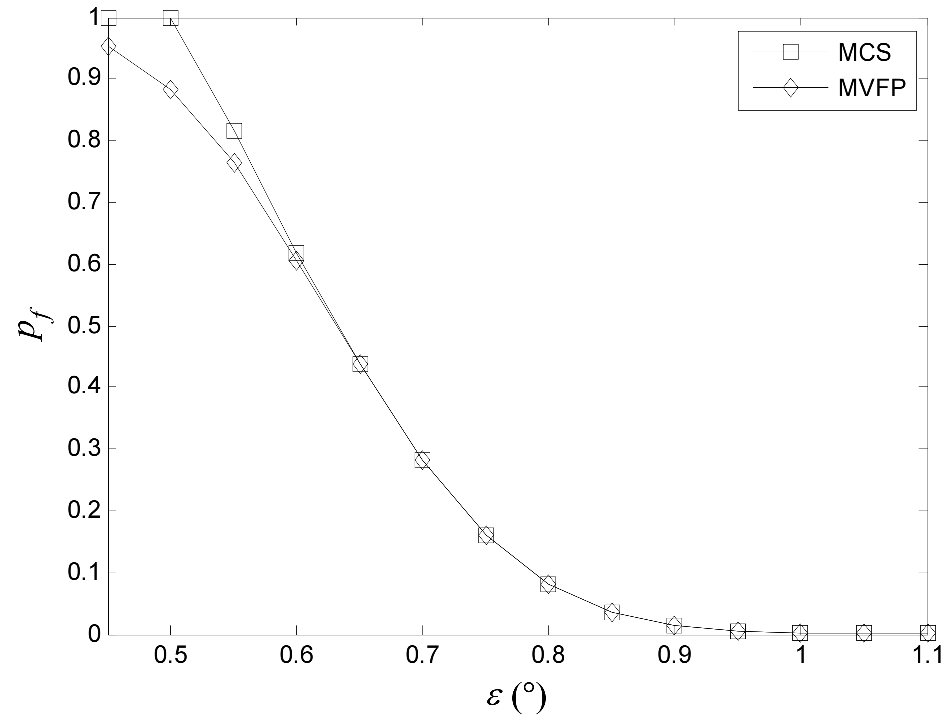

Fig. 6 p_f **of the log function generator (case 1)**

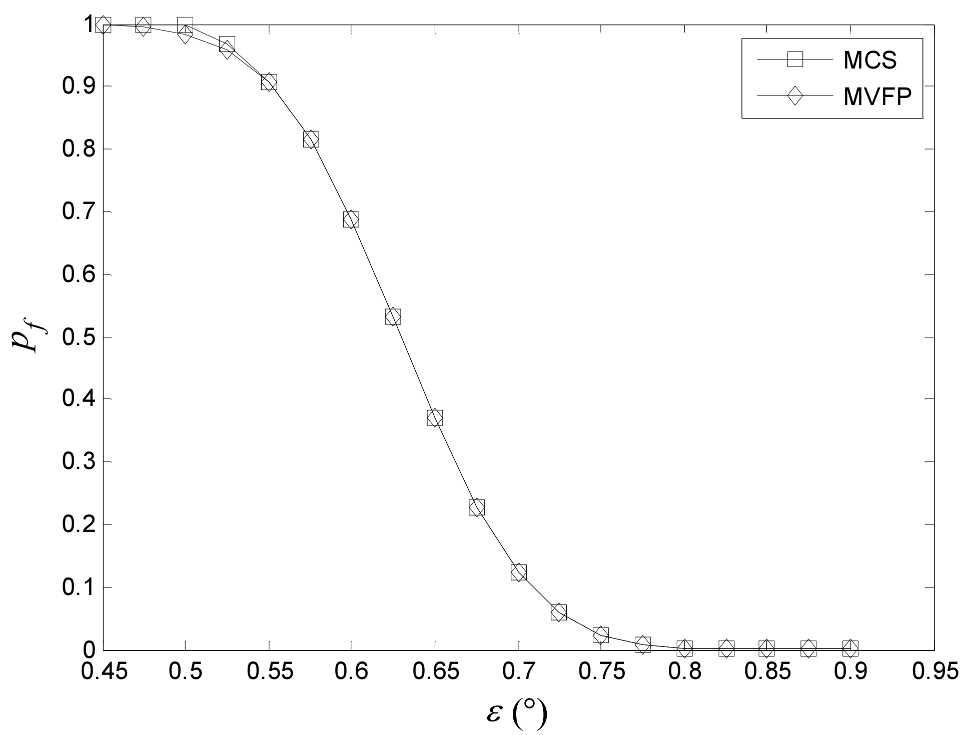

Fig. 7 p_f **of the log function generator (Case 2)**

5 Conclusions

For function generator mechanisms, time-dependent kinematic reliability is more critical than point kinematic reliability. The reason is that the former reliability provides complete information about the likelihood of the desired function being realized over the entire motion range of interest while the latter reliability only gives the instantaneous likelihood at a specific time instant.

This work develops an analysis method for the time-dependent kinematic reliability for function generator mechanisms. The method extends the First Order Second Moment (FOSM) method to time-dependent problems using the concepts of upcrossing and downcrossing. Analytical upcrossing and downcrossing rates are available with the proposed method. The method can assess the time-dependent reliability by accounting for both the structural error (bias) and mechanical (random) error. Although the method is demonstrated with a planar mechanism, it is also applicable for spatial mechanisms.

The method is accurate with small dimension tolerances, which is the case in most engineering applications. The method is also efficient because the analytical equations of the upcrossing and downcrossing rates are available. There is no need to use any random sampling such as Monte Carlo simulation or any iterative processes.

The method may not be accurate when the standard deviations of dimension variables are high; for example, the standard deviation of a dimension variable is greater than 10% of its mean. Inaccuracy also occurs when the reliability of the mechanism is too low. This is caused by the Poisson approximation.

Possible future work includes the following topics: (1) Introduce the method into reliability-based mechanism synthesis. (2) Consider random clearance variables for the joints of a mechanism. (3) Extend the present method to other types of mechanisms, such as path generator mechanisms.

Acknowledgement

We would like to thank the financial support from Xihua University to the first author for his stay as a Visiting Scholar at the Missouri University of Science and Technology (MST). We would also like to acknowledge the support from the Intelligent Systems Center at MST for the second author and the support from the Key Lab of Manufacturing and Automation of Sichuan Province at Xihua University for the first author.

References

[1] Issac, K. K., 1993, "A Nondifferentiable Optimization Algorithm for Constrained Minimax Linkage Function Generation," Journal of Mechanical Design 115(4), pp. 978-988.

[2] Aviles, J. V., Hernández, A., and Amezua, E., 1995, "Nonlinear Optimization of Planar Linkages for Kinematic Syntheses, " Mechanism and Machine Theory, 30(4), pp. 501-518.

[3] Simionescu, P. A., and Beale, D., 2002, "Optimum Synthesis of the Four-Bar Function Generator in Its Symmetric Embodiment: The Ackermann Steering Linkage," Mechanism and Machine Theory, 37(12), pp. 1487-1504

[4] Mariappan, J., and Krishnamurty, S., 1996, "A Generalized Exact Gradient Method for Mechanism Synthesis," Mechanism and Machine Theory, 31(4), pp. 413-421.

[5] Rao, A. C., 1979, "Synthesis of 4-Bar Function-Generators Using Geometric Programming," Mechanism and Machine Theory, 14(2), pp. 141-149.

[6] Mallik, A. K., Ghosh, A., and Dittrich, G., 1994, *Kinematic Analysis and Synthesis of Mechanisms*, CRC-Press.

[7] Zhu, J., and Ting, K.-L., 2000, "Uncertainty Analysis of Planar and Spatial Robots with Joint Clearances," Mechanism and Machine Theory, 35(9), pp. 1239-1256.

[8] J.R. Baumgarten, and Werff, K. V. D., 1985, "A Probabilistic Study Relating to Tolerancing and Path Generation Error," Mechanism and Machine Theory 20(1), pp. 71-76.

[9] S.G. Dhande, J. C., 1973, " Analysis and Synthesis of Mechanical Error in Linkages – a Stochastic Approach," Journal of Engineering for Industry, Transactions of the ASME, 95(3), pp. 672-676.

[10] Wei-Liang, X., and Qi-Xian, Z., 1989, "Probabilistic Analysis and Monte Carlo Simulation of the Kinematic Error in a Spatial Linkage," Mechanism and Machine Theory, 24(1), pp. 19-27.

[11] Dubowsky, S., Norris, M., Aloni, M., and Tamir, A., 1984, "An Analytical and Experimental Study of the Prediction of Impacts in Planar Mechanical Systems with Clearances," ASME Journal of Mechanisms, Transmissions, 106(4), pp. 444-451.

[12] Parenti-Castelli, V., and Venanzi, S., 2005, "Clearance Influence Analysis on Mechanisms," Mechanism and Machine Theory, 40(12), pp. 1316–1329.

[13] Tsaia, M.-J., and Lai, T.-H., 2008, "Accuracy Analysis of a Multi-Loop Linkage with Joint Clearances," Mechanism and Machine Theory, 43(9), pp. 1141-1157.

[14] Zhen, H., 1987, "Error Analysis of Position and Orientation in Robot Manipulators," Mechanism and Machine Theory, 22(6), pp. 577-581.

[15] Rajagopalan, S., and Cutkosky, M., 2003, "Error Analysis for the in-Situ Fabrication of Mechanisms," Journal of Mechanical Design, 125(4), pp. 809-822.

[16] Sergeyev, V. I., 1974, "Methods for Mechanism Reliability Calculation," Mechanism and Machine Theory, 9(1), pp. 97-106.

[17] Bhatti, P., 1989, "Probabilistic Modeling and Optimal Design of Robotic Manipulators," Ph.D. thesis, Purdue University, West Lafayette, Indiana.

[18] Shi, Z., Yang, X., Yang, W., and Cheng, Q., 2005, "Robust Synthesis of Path Generating Linkages," Mechanism and Machine Theory, 40(1), pp. 45-54.

[19] Shi, Z., 1997, "Synthesis of Mechanical Error in Spatial Linkages Based on Reliability Concept," Mechanism and Machine Theory, 32(2), pp. 255-259.

[20] Du, X., Venigella, P. K., and Liu, D., 2009, "Robust Mechanism Synthesis with Random and Interval Variables," Mechanism and Machine Theory, 44(7), pp. 1321-1337.

[21] Du, X., 1996, "Reliability Synthesis for Mechanism," Machine Design 13(1), pp. 8-11(in chinese).

[22] Rao, S. S., and Bhatti, P. K., 2001, "Probabilistic Approach to Manipulator Kinematics and Dynamics," Reliability Engineering & System Safety, 72(1), pp. 47-58.

[23] Liu, T. S., and Wang, J. D., 1994, "A Reliability Approach to Evaluating Robot Accuracy Performance," Mechanism and Machine Theory, 29(1), pp. 83-94.

[24] Bhatti, P. K., and Rao, S. S., 1988 "Reliability Analysis of Robot Manipulators," TRANS. ASME J. MECH. TRANSMISSIONS AUTOM, 110(2), pp. 175-181.

[25] Kim, J., Song, W.-J., and Kang, B.-S., 2010, "Stochastic Approach to Kinematic Reliability of Open-Loop Mechanism with Dimensional Tolerance," Applied Mathematical Modelling 24(5), pp. 1225-1237.

[26] Bowlin, A. P., Renaud, J. E., Newkirk, J. T., and Patel, N. M., 2007, "Reliability-Based Design Optimization of Robotic System Dynamic Performance," Journal of Mechanical Design 129(4), pp. 449-455.

[27] Yaofei, T., Jianjun, C., Chijiang, Z., and Yongqin, C., 2007, "Reliability Analysis of Kinematic Accuracy for the Elastic Slider-Crank Mechanism," Frontiers of Mechanical Engineering in China, 2(2), pp. 214-217.

[28] L. L. Howell, Rao, S. S., and Midha, A., 1994, "Reliability-Based Optimal Design of a Bistable Compliant Mechanism," Journal of Mechanical Design 116(4), pp. 1115 -221.

[29] Shu, C. H., and Radcliffe, C. W., 1987, *Kinematics and Mechanism Design*, John Wiley & Sons, Inc.

[30] Sudret, B., 2008, "Analytical Derivation of the Outcrossing Rate in Time-Variant Reliability Problems," Structures and Infrastructure Engineering, 4(5), pp. 353-362.

[31] Li, J., Chen, J.-B., and Fan, W.-L., 2007, "The Equivalent Extreme-Value Event and Evaluation of the Structural System Reliability," Structural Safety, 29(2), pp. 112-131.

[32] Chen, J.-B., and Li, J., 2007, "The Extreme Value Distribution and Dynamic Reliability Analysis of Nonlinear Structures with Uncertain Parameters," Structural Safety, 29(2), pp. 77-93.

[33] Lutes, L. D. A. S., S, 2004, *Random Vibrations: Analysis of Structural and Mechanical Systems*, Elsevier Butterworth Heinemann.

[34] Lutes, L. D., and Sarkani, S., 2009, "Reliability Analysis of Systems Subject to First-Passage Failure," Technical Report No. NASA/CR-2009-215782, NASA Langley Research Center.

[35] Li, J., and Mourelatos, Z. P., 2009, "Time-Dependent Reliability Estimation for Dynamic Problems Using a Niching Genetic Algorithm," Journal of Mechanical Design 131(7), pp. 1009 -1022.

[36] Li, C. C., and Der-Kiureghian, A., 1995, "Mean out-Crossing Rate of Nonlinear Response to Stochastic Input," L. M, et al., eds., Paris, France, pp. 295-302.

[37] Breitung, K., 1988, "Asymptotic Crossing Rates for Stationary Gaussian Vector Processes," Stochastic Processes and their Applications 29 (2), pp. 195-207.

[38] K, B., 1993, "Asymptotic Approximations for the Crossing Rates of Poisson Square Waves," eds., Gaithersburg/Maryland, 3, pp. 75-80.

[39] Rackwitz, R., 1997, Probabilistic Methods for Structural Design, Kluwer Academic Publishers, Time-Variant Reliability for Non-Stationary Processes by the Outcrossing Approach.

[40] Schrupp, K., and Rackwitz, R., 1988, "Outcrossing Rates of Marked Poisson Cluster Processes in Structural Reliability," Applied Mathematical Modelling, 12(5), pp. 482-490.

[41] Andrieu-Renaud, C., Sudret, B., and Lemaire, M., 2004, "The Phi2 Method: A Way to Compute Time-Variant Reliability," Reliability Engineering & System Safety, 84(1), pp. 2004.

[42] Hagen, O., and Tvedt, L., 1991, "Vector Process out-Crossing as Parallel System Sensitivity Measure," Journal of Engineering Mechanics, 117(10), pp. 2201-2220.

[43] Rice, S. O., 1944, "Mathematical Analysis of Random Noise," Bell Systems Technical Journal, 23,pp. 282-332.

[44] Middleton, D., 1960, *An Introduction to Statistical Communication Theory*, McGraw-Hill, New York.

[45] Rackwitz, R., 2001, "Reliability Analysis—a Review and Some Perspectives," Structural Safety, 23(4), pp. 365-395.

[46] Leishman, R. C., and Chase, K. W., 2010, "Direct Linearization Method Kinematic Variation Analysis," Journal of Mechanical Design, 132(7), pp. 1003(1-9).